ELSEVIER

Materials Science and Engineering A341 (2003) 273–281

MATERIALS SCIENCE & ENGINEERING A

www.elsevier.com/locate/msea

High strain rate superplasticity of submicrometer grained 5083 Al alloy containing scandium fabricated by severe plastic deformation

Kyung-Tae Park [a,*], Duck-Young Hwang [a], Young-Kook Lee [b], Young-Kuk Kim [c], Dong Hyuk Shin [c]

[a] Division of Advanced Materials Science and Engineering, Hanbat National University, Taejon 305-719, Republic of Korea
[b] Department of Metallurgical Engineering, Yonsei University, Seoul 120-749, Republic of Korea
[c] Department of Metallurgy and Materials Science, Hanyang University, Ansan 425-791, Republic of Korea

Received 16 November 2001; received in revised form 8 April 2002

Abstract

High strain rate superplasticity (HSRS) was obtained in a commercial 5083 Al alloy by introducing a ultrafine grained structure of 0.3 μm through severe plastic deformation and by adding a dilute amount of scandium (Sc) as a microstructure stabilizer. Tensile tests were carried out on the as-processed sample at temperatures of 623–823 K and initial strain rates of 1×10^{-3}–1×10^{0} s^{-1}. The maximum elongation to failure of 740% was obtained at 773 K and 1×10^{-2} s^{-1}. HSRS of the alloy was attributed to the combined effects of dynamic recrystallization and preservation of fine recrystallized grains by the presence of Sc. The mechanical behavior of the alloy at 773 K was characterized by a sigmoidal behavior in a plot of stress vs strain rate in the double logarithmic scale. The origin of the sigmoidal behavior was discussed in terms of microstructural evolution during superplastic deformation. An examination of the fractured samples revealed that failure occurred in a brittle manner related to cavitation rather than necking. Cavity stringers were formed parallel to the tensile axis by interlinkage of jagged-shaped isolated cavities along grain boundaries aligned to the tensile axis.

Keywords: High strain rate superplasticity; 5083 Al alloy; Scandium; Severe plastic deformation; Ultrafine grains

1. Introduction

Of many superplastic Al alloys developed, the Al–Mg based 5083 Al alloy is one of the most widely used alloys for commercial superplastic forming. This is because the 5083 Al alloy possesses many interesting characteristics as a structural material such as low price, moderate strength, good corrosion resistance, high formability in conjunction with moderate superplasticity [1]. Naturally, numerous investigations [2–7] have been conducted to enhance the superplastic properties of the alloy. For instance, Gosh and coworkers [2] obtained an elongation of 670% in the alloy under conditions of the grain size = 9 μm, $T = 798$ K, strain rate = 1×10^{-3} s^{-1}, and a hydrostatic back pressure = 5.5 MPa. This may be the largest elongation ever reported for commercial 5083 Al alloy. Meanwhile, a recent progress of low temperature and/or high strain rate superplasticity (HSRS) along with the emergence of the new techniques processing ultrafine grained materials provides a breakthrough to overcome the current limit of conventional superplasticity, i.e. high forming temperature and slow forming rate. In this regard, for the 5083 Al alloy, little information on HSRS is available at present while many researches have been conducted for achieving conventional superplasticity and low temperature superplasticity as summarized by Hsiao and Huang [8].

In the present investigation, an attempt was made to obtain HSRS in the 5083 Al alloy by adopting two approaches, i.e. an introduction of a ultrafine grained structure through equal channel angular pressing (ECAP) and an addition of a small amount of scandium (Sc). ECAP is, at present, the most developed severe plastic deformation technique producing bulk, porosity-

* Corresponding author. Tel.: +82-42-821-1243; fax: +82-42-821-1592
E-mail address: ktpark@tunt.ac.kr (K.-T. Park).

0921-5093/02/$ - see front matter
PII: S0921-5093(02)00216-2

free ultrafine grained materials, which are suitable for superplasticity. In ECAP, an ultrafine grained structure is obtained via mechanical fragmentation associated with severe plastic deformation by subjecting the sample to repetitive pressing into a die with the two equal cross-sectional channels intersecting at a certain angle [9,10]. However, ultrafine grained materials fabricated by ECAP exhibited enhanced grain growth behavior at thermal exposure due to accumulation of large plastic strain inside materials [11], deteriorating superplasticity during high temperature deformation. Accordingly, an addition of alloying element stabilizing an ultrafine grained structure is essential to achieve a desired HSRS in ECAPed ultrafine grained materials. In this study, Sc was selected as a microstructure stabilizer since it is known to be the most effective on suppressing recrystallization of severely worked Al alloys as well as increasing the strength among any alloying elements for Al alloys on an equal atomic fraction basis [12–14].

2. Experimental procedure

The present alloy was prepared by a squeeze-casting method in order to minimize undesired shrinkage and gaseous porosity. A commercial 5083 Al alloy was remelted with an addition of a proper amount of Al–2wt.%Sc master alloy. The melt was poured into a preheated mold at 983 K and was squeeze-cast under an applied pressure of 100 MPa, a plunger speed of 23 mm s^{-1}, and a mold temperature of 523 K. The final chemical composition was Al–4.2Mg–0.6Mn–0.1Cr–0.2Sc (in wt.%). The squeeze-cast alloy was homogenized at 753 K for 24 h and then was machined the cylindrical bars of ϕ 50 mm × 100 mm for the subsequent hot extrusion. Hot extrusion was carried out at 683 K with the extrusion ratio of 17:1 and an extrusion speed of 7 mm s^{-1}. After hot extrusion, the alloy was annealed at 843 K for 1 h.

After machining the cylindrical sample of ϕ 10 mm × 130 mm from the extruded bar, ECAP was conducted at 473 K with a die designed to yield an effective strain of ~1 by a single pass: inner contact angle and the arc of curvature at the outer point of contact between channels of the die were 90 and 20°, respectively. ECAP was performed up to 4-passes, i.e. accumulated strain of ~4, by rotating the sample 90° around its longitudinal axis in the same direction between the passages, i.e. route B_c [15]. The detailed ECAP procedure and facility were described elsewhere [16].

The microstructural stability of the ECAPed alloy was examined by conducting static annealing at temperatures of 373–773 K for 1 h in a silicone oil bath and a salt bath and by measuring the microhardness value. During annealing, the temperature was controlled within ±1 K. In order to recognize the effect of Sc addition on thermal stability of the alloy, the identical squeeze-casting, ECAP, static annealing and the microhardness measurement were conducted on the alloy without Sc. For superplastic deformation, tensile specimens with a gage length of 8 mm were machined from the as-ECAPed bar. Tensile tests were carried out at the initial strain rates of 10^{-3}–10^{0} s^{-1} and temperatures of 623–823 K on an Instron machine operating at a constant rate of crosshead displacement. The selection of the testing temperature will be addressed in Section 3. All the tests were performed in a three-zone furnace in air. The heating time to the desired testing temperature was approximately 30 min and the sample was held about 10 min before starting the test to reach a thermal equilibrium. The testing temperature was controlled within ±3 K.

The microstructure was examined using a JEOL 2010 transmission electron microscope (TEM) operating at 200 kV. Thin foils for TEM observation were prepared by a twin-jet polishing technique using a mixture of 25% nitric acid and 75% methanol at an applied potential of 25 V and at 243 K. In addition, the grain structure and cavitation after failure were observed by optical microscope (OM) after etching with a dilute Poulton's reagent.

3. Results

3.1. Thermal stability and microstructure of the ECAPed 5083 Al with Sc

Fig. 1 shows the microhardness variation with annealing temperature for 1 h static annealing. For the 5083 Al

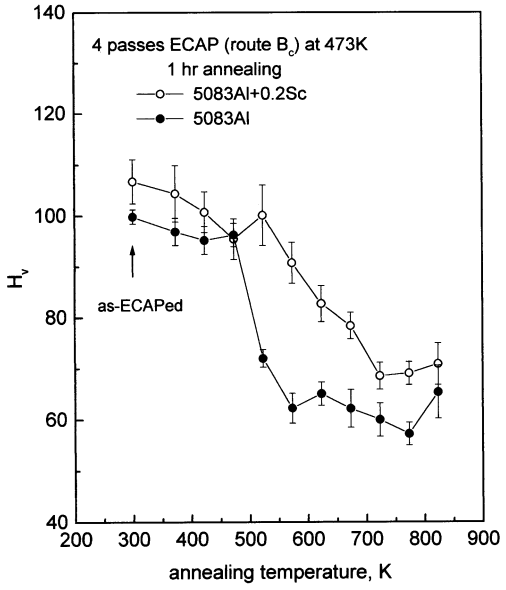

Fig. 1. Microhardness variation of the ECAPed 5083Al+0.2Sc alloy with annealing temperature (annealing time = 1 h).

alloy with Sc (5083Al+0.2Sc), the hardness did not change significantly up to 523 K. Then, it decreased gradually in the temperature range of 523–723 K due to recovery and recrystallization. Above 723 K, the hardness remained the same. For the alloy without Sc, the hardness started to decrease from 473 K. On the contrary to a gradual hardness decrease of the 5083Al+0.2Sc alloy in a relatively wide range of temperature, the alloy without Sc exhibited a rapid hardness loss in the narrow temperature range of 473–523 K. The above finding clearly showed the retardation effect of Sc against recovery and recrystallization. In addition, the absolute hardness value of the 5083Al+0.2Sc alloy was higher than that of the alloy without Sc at all annealing temperatures.

The representative TEM microstructures of the as-ECAPed and annealed samples are shown in Fig. 2. As typical in ultrafine grained materials processed by severe plastic deformation [10,11,16], the as-ECAPed sample (Fig. 2a) exhibited ill-defined boundaries, high dislocation density with dense dislocation debris, extensive extinction contours in the vicinity of boundaries, etc. The grain size was about 0.3 μm. At 423 K, where no significant microhardness loss occurred, the microstructure (Fig. 2b), was virtually the same with that of the as-ECAPed sample. The microstructure of the sample annealed at 623 K which belonged to the temperature range showing a gradual microhardness loss consisted of unrecrystallized ultrafine grains (upper half part of Fig. 2c) and coarse recrystallized grains (lower half part of Fig. 2c). As marked by arrows, grain boundaries of unrecrystallized ultrafine grains were pinned by the extremely fine second phase particles. At 723 K with the low microhardness value, homogeneous distribution of coarse grains with an average size of 8 μm was the main feature of the microstructure due to grain growth following recrystallization (Fig. 2d).

The enhanced thermal stability and hardness resulted from the effect of Sc as a microstructure stabilizer and a strengthener associated with precipitation of stable Al_3Sc particles [12,17–20]. As shown in Fig. 3a, the Al_3Sc particles existed as an extremely fine, typically 10–50 nm, and spherical form in the sample annealed at 773 K for 1 h. As discussed later, 773 K was determined to be the optimum HSRS temperature of the alloy under the present experimental conditions. Besides, since the deformation time for HSRS is usually shorter than 1 h, the size of the Al_3Sc particles is expected to be smaller

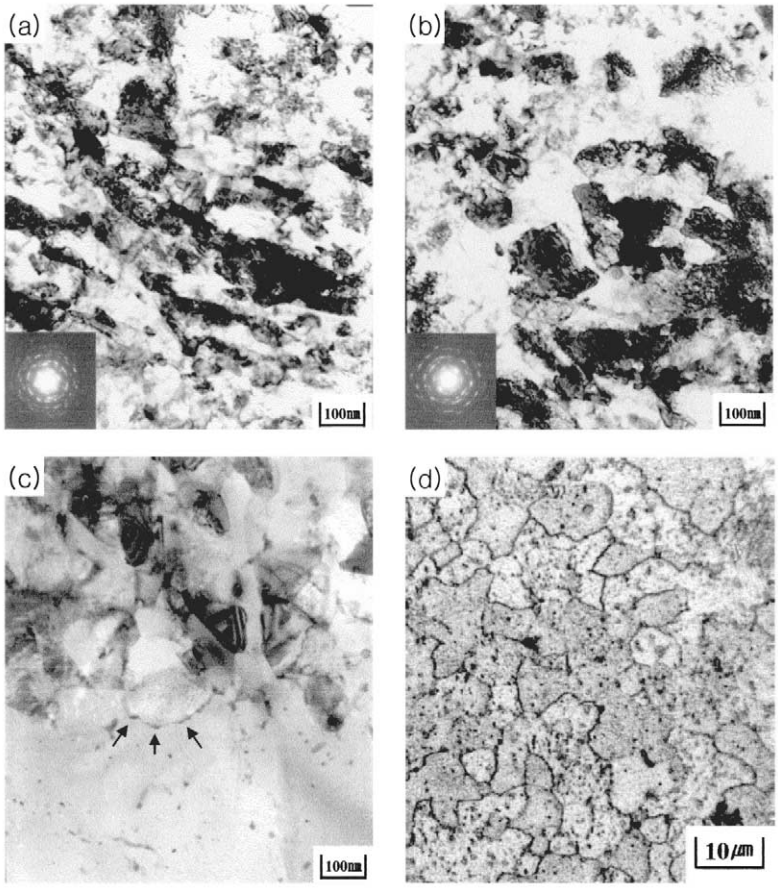

Fig. 2. Microstructures of the ECAPed 5083Al+0.2Sc alloy after 1 h static annealing at various temperatures. (a) as-ECAPed (TEM); (b) 423 K (TEM); (c) 623 K (TEM); (d) 723 K (OM).

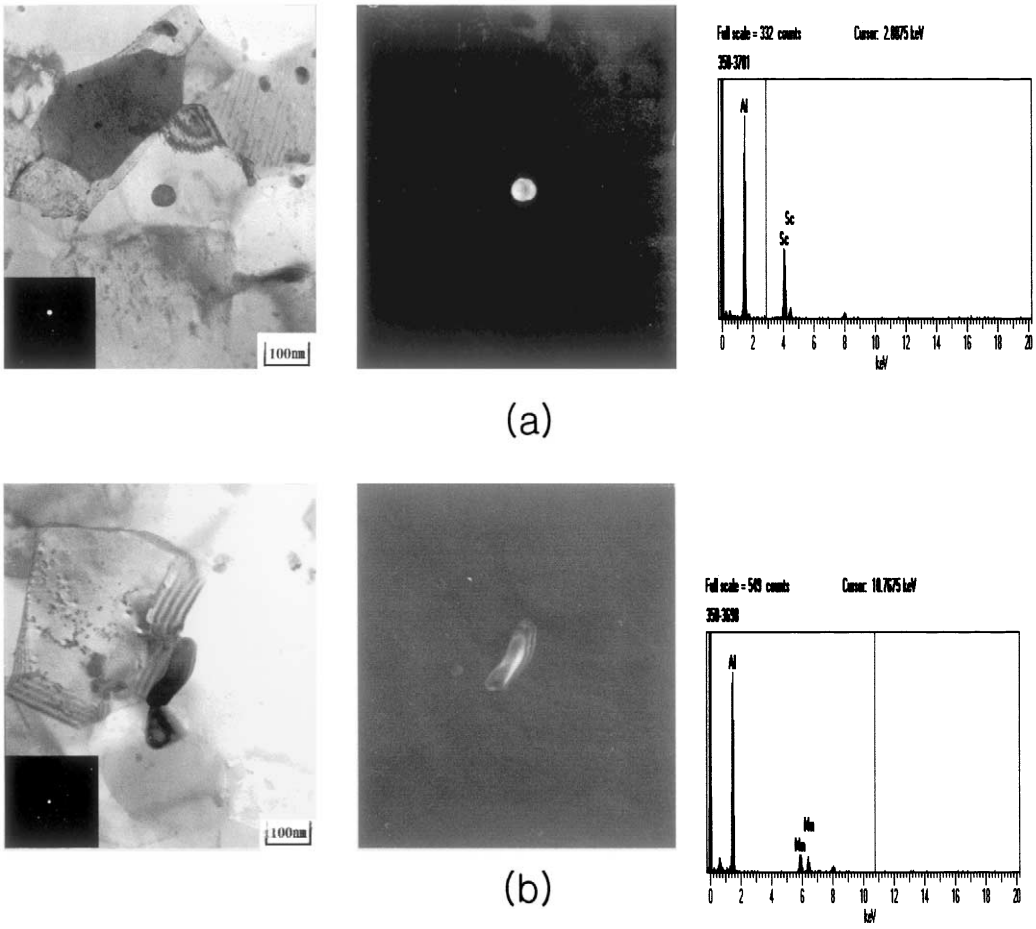

Fig. 3. The bright and dark field images of TEM and the energy dispersive spectra of the particles in the ECAPed 5083Al+0.2Sc alloy annealed at 773 K for 1 h. (a) Al_3Sc; (b) Al_6Mn.

than that shown in Fig. 3a during HSRS experiment. In addition to the Al_3Sc particles, the Mn-rich particles known as Al_6Mn [2] were also observed (Fig. 3b). The Mn-rich particles are the primary second phase particles in the 5083 Al alloy and are easily distinguished from the Al_3Sc particles in terms of the shape and size. The size and aspect ratio of the Mn-rich particles were about 0.2 μm and 4, respectively, in the present 5083Al+Sc alloy.

3.2. HSRS characteristics

3.2.1. Optimum HSRS temperature

In order to determine the optimum HSRS temperature, the tensile tests were carried out on the as-ECAPed 5083Al+0.2Sc samples at an initial strain rate of 1×10^{-2} s^{-1} in the temperature range of 623–823 K with 50 K interval. HSRS has been defined as a superplastic behavior at the strain rate of 1×10^{-2} s^{-1} or faster by Japanese Standards Association (JIS H 7007) [21]. The temperature range of 623–823 K was selected by the following considerations. First, without the accommodation helper for grain boundary sliding such as the thin liquid phase layer at the grain boundaries associated with a partial melting [22], the ultrafine grain size with high angle grain boundaries is a necessary condition for achieving HSRS. A number of previous studies [23,24] revealed that a large portion of grain boundaries of the as-ECAPed metals and alloys is low-angled. Accordingly, the formation of high angle grain boundaries is required through either static or dynamic recrystallization. The 5083Al+0.2Sc alloy exhibited the occurrence of recovery and recrystallization at temperatures of 523–723 K in 1 h static annealing as discussed in the preceding section. However, the present heating condition before starting the test, i.e. ~30 min heating and ~10 min holding, was shorter than 1 h. Therefore, higher temperatures in this temperature range seemed to be beneficial to form high angle grain boundaries and so the test was carried out from 623 K. Second, 823 K that is ~30 K lower than the incipient melting temperature, 857 K (Fig. 4) was determined as the highest testing temperature in order to ensure no presence of the liquid phase.

Fig. 5 presents the elongation to failure, e_f, of the as-ECAPed 5083Al+0.2Sc alloy as a function of the testing temperature. While the e_f at the lowest and

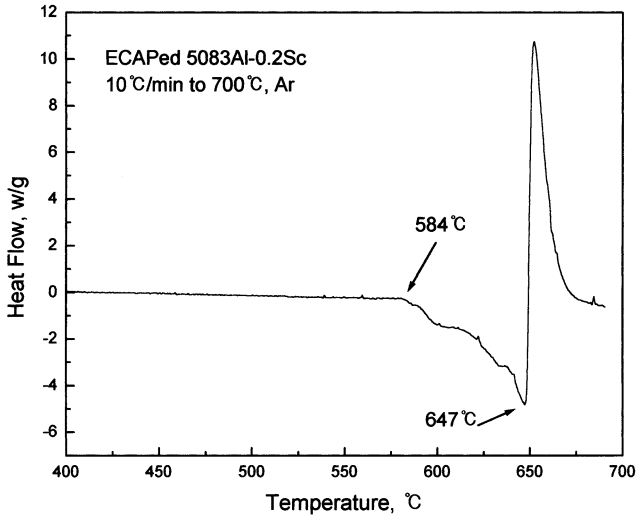

Fig. 4. The differential scanning calorimetry profile of the ECAPed 5083Al+0.2Sc alloy showing the occurrence of a partial melting at 857 K (heating rate = 10 K min^{-1}).

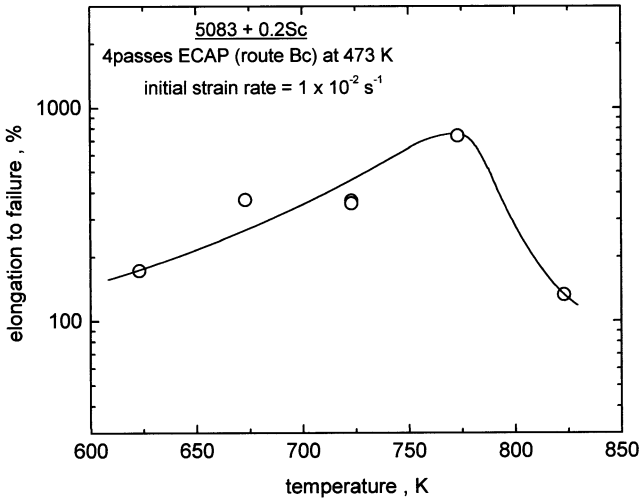

Fig. 5. The elongation to failure of the as-ECAPed 5083Al+0.2Sc alloy as a function of testing temperature at the initial strain rate of 1×10^{-2} s^{-1}.

highest testing temperatures was less than 200%, it was over 300% at temperatures of 673–773 K with the maximum e_f of 740% at 773 K. In Fig. 6, the microstructures of the grip and gage sections of the sample tested at the initial strain rate of 1×10^{-2} s^{-1} and 773 K are shown. The optical microstructure of the grip section (Fig. 6a) consisted of unrecrystallized elongated structure inclined 30° to the tensile or the longitudinal axes of the sample. This microstructural alignment resulted from the shear characteristics of ECAP. The theoretical shear angle with respect to the longitudinal axis of the sample is about 26.5° when the inner and outer contact angles between the two channels of the ECAP die are 90 and 20°, respectively [25]. However,

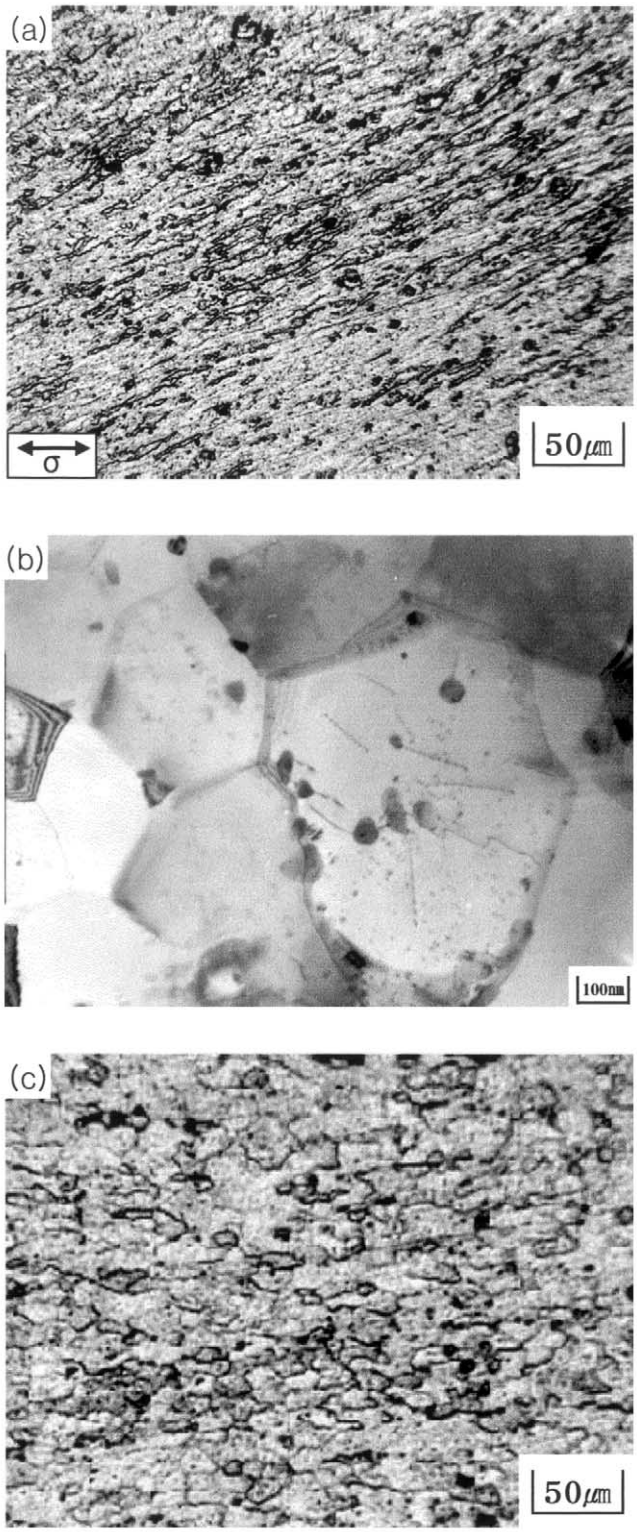

Fig. 6. Microstructures of the as-ECAPed 5083Al+Sc alloy tested at the initial strain rate of 1×10^{-2} s^{-1} and 773 K. (a) The grip section (OM); (b) the grip section (TEM); (c) the gage section (OM).

under TEM observation, the microstructure of the grip section (Fig. 6b) was characterized by recovered ultrafine grains. It was noted that many grain boundaries of

recovered grains were pinned by extremely fine Al_3Sc particles of which size and shape were similar to those shown in Fig. 3a. By contrast, the microstructure of the gage section (Fig. 6c) was manifested by the homogeneous distribution of fairly equiaxed grains of ~ 5 μm. From the comparison of the microstructure between the grip and gage sections, it is obvious that dynamic recrystallization during tensile deformation is responsible for HSRS of the present as-ECAPed 5083Al+0.2Sc alloy. The lowest testing temperature of 623 K might be too low for dynamic recrystallization to occur and then low e_f was resulted. The low e_f at the highest testing temperature of 823 K was definitely due to excessive grain growth since the grain size of the grip section of the sample was measured as ~ 30 μm.

3.2.2. Mechanical behavior at 773 K

The mechanical behavior of the as-ECAPed 5083Al+0.2Sc alloy at the optimum superplastic temperature, i.e. 773 K, was examined by testing the samples at various strain rates ranged from 10^{-3} to 10^{0} s^{-1} and by plotting the maximum true flow stress as a function of the true strain rate in a double logarithmic scale. Such a plot is depicted in Fig. 7. A sigmoidal behavior, which is typically observed in conventional superplastic materials, was evident. While the strain rate sensitivity, m, was about 0.25 at the high and low strain rate regions, it was 0.5 at the intermediate strain rate region, indicating an operation of the grain boundary sliding mechanism. It is noted that the intermediate strain rate region of $m = 0.5$ was relatively narrow, covering only one order of magnitude of strain rate.

The e_f at 773 K is plotted as a function of the initial strain rate in Fig. 8a. The e_f was less than 300% at the low and high strain rate regions due to the low value of

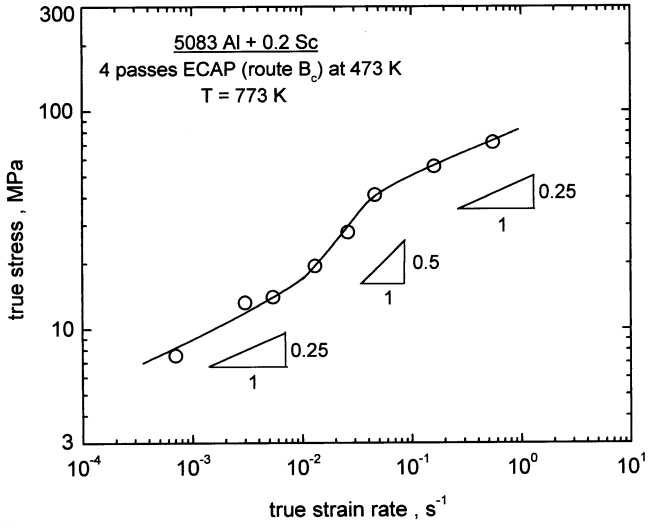

Fig. 7. A plot of the maximum true flow stress against the true strain rate in a double logarithmic scale for the as-ECAPed 5083Al+0.2Sc alloy at 773 K.

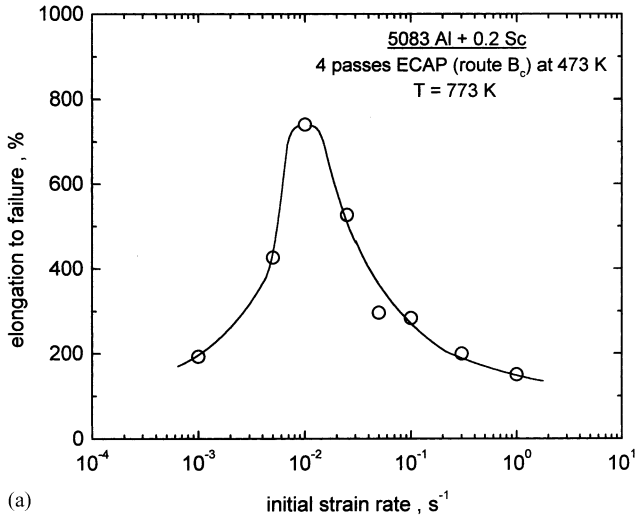

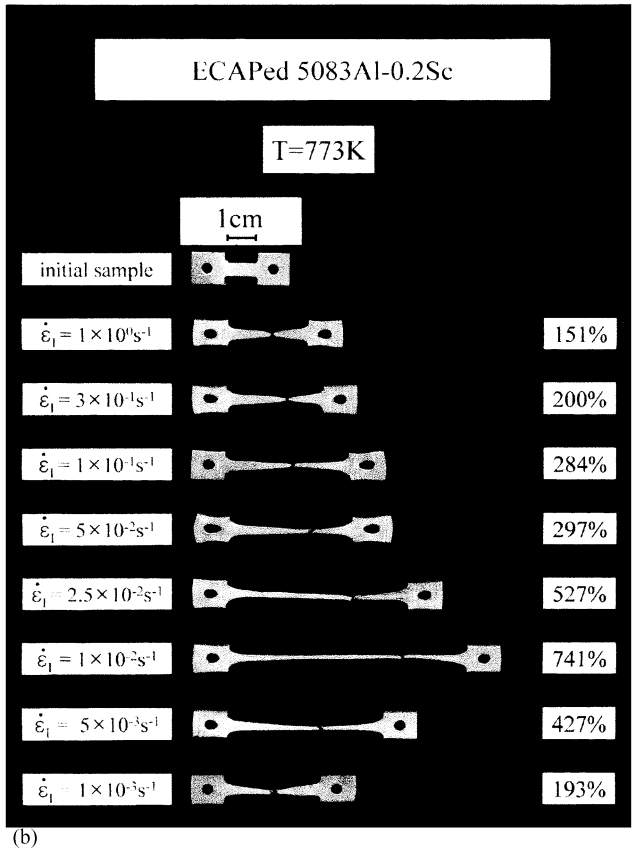

Fig. 8. (a) The elongation to failure of the as-ECAPed 5083Al+0.2Sc alloy as a function of the initial strain rate at 773 K. (b) An appearance of the fractured samples of the as-ECAPed 5083Al+0.2Sc alloy tested at 773 K.

m. However, the e_f was higher than 400% at the strain rates of 5×10^{-3}–2.5×10^{-2} s^{-1}, corresponding to the intermediate strain rate region of $m = 0.5$, with the maximum e_f of 740% at the initial strain rate of 1×10^{-2} s^{-1}. The fractured samples tested at the various initial strain rates at 773 K are shown in Fig. 8b.

Necking was visible in the sample pulled to failure at the high strain rates. On the contrary, the samples were fractured abruptly in a brittle manner with negligible necking at the intermediate and low strain rate regions, suggesting that cavitation played a major role on the abrupt failure. The optical micrographs of the polished gage section of the sample tested at the initial strain rate of $1 \times 10^{-2}\ s^{-1}$ and 773 K are shown in Fig. 9. Cavities were developed in a jagged configuration and the cavity interlinkage seemed to occur along the grain boundaries parallel to the tensile axis. The formation of cavity stringer parallel to the tensile axis is more evident in the micrograph taken from the same sample after etching (Fig. 10). The cavity stringer alignment along the tensile axis is commonly observed in the quasi-single phase superplastic alloys containing fine second phase particles as a microstructure stabilizer [26–29]. This is often explained as a result of alignment of the particles along the working direction, such as rolling, during materials preparation and their role providing the favorable cavity nucleation site. However, this explanation cannot be applied to the present case since, as mentioned in Fig. 6, the final shear direction in ECAP is about 30° inclined to the longitudinal axis of the sample. Instead, the microstructural evolution associated with dynamic recrystallization during testing is expected to play a dominant role on the cavity stringer formation along the tensile axis.

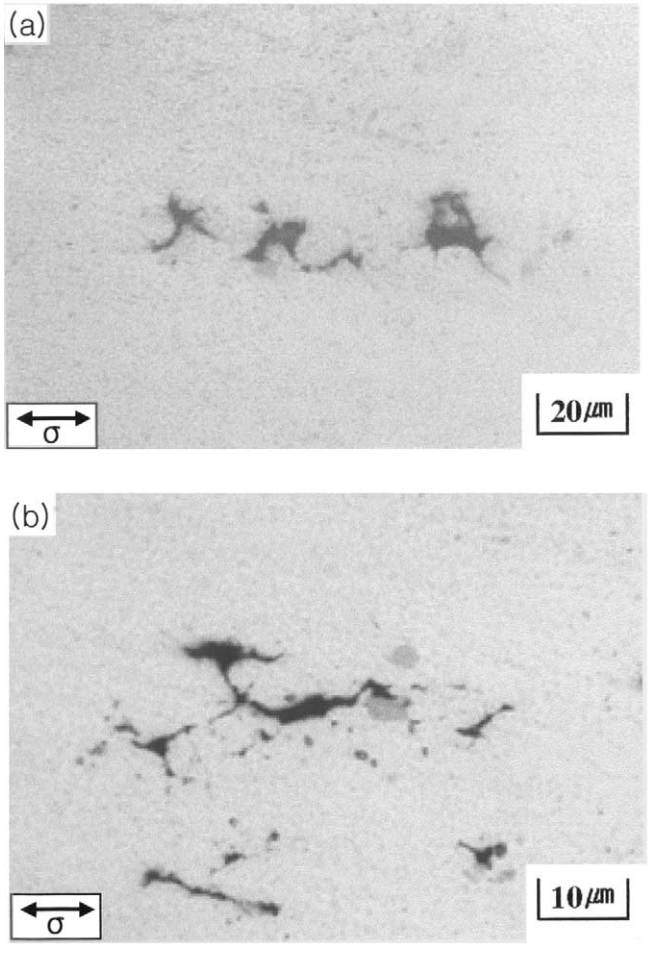

Fig. 9. The cavity configuration developed in the as-ECAPed 5083Al+0.2Sc alloy tested at 773 K and $1 \times 10^{-2}\ s^{-1}$. (a) Isolated cavities with jagged configuration; (b) cavity interlinkage along the grain boundaries.

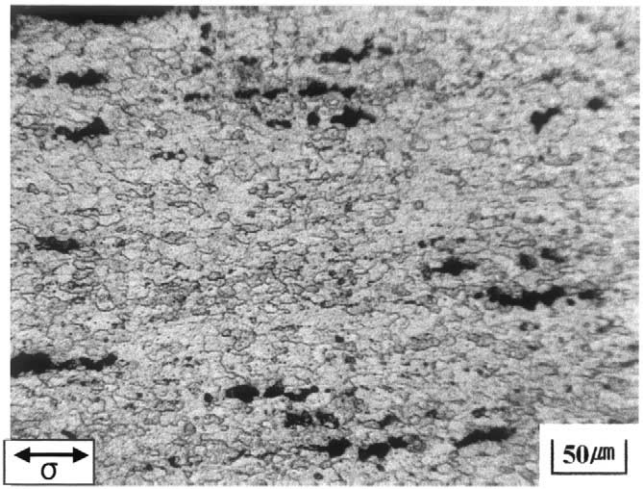

Fig. 10. The presence of cavity stringers parallel to the tensile axis in the as-ECAPed 5083Al+0.2Sc alloy tested at 773 K and $1 \times 10^{-2}\ s^{-1}$.

4. Discussion

4.1. HSRS of submicrometer grained ECAPed 5083Al+Sc

The present experimental results showed the occurrence of the optimum HSRS at the temperature of 773 K and the narrow strain rate range of 5×10^{-3}–$2.5 \times 10^{-2}\ s^{-1}$ for the submicrometer grained 5083Al+0.2Sc alloy fabricated by 4-passes ECAP with route B_c. In addition, the mechanical behavior was manifested by a sigmoidal behavior in a double logarithmic plot of the maximum true flow stress vs the true strain rate.

As illustrated in Fig. 6, the occurrence of HSRS of the present alloy at the intermediate strain rate region was attributed to dynamic recrystallization. A large portion of the grain boundaries of the as-ECAPed alloy was low-angled. The grain boundaries of fresh recrystallized grains formed by dynamic recrystallization during deformation are high-angled and, therefore, they are suitable for grain boundary sliding characterized by $m = 0.5$. In addition, the recrystallized grains remained fine, typically less than 5 μm as shown in Fig. 6c, by the presence of stable, fine Al_3Sc particles. The microstructure, which resulted from these combined effects, satisfied the microstructural prerequisites for superplasticity.

For the low value of m at the high strain rate region, two possibilities can be considered. First, Sherby and Burke [30] proposed that power law breakdown in high temperature deformation of FCC materials occurs at a diffusivity normalized strain rate of $\dot{\varepsilon}/D = 10^{13}$ m^{-2} where $\dot{\varepsilon}$ is the strain rate and D is the diffusivity. Accordingly, it is worth examining whether the experiment was carried out in the power law breakdown region. When $D = 1.24 \times 10^{-4} \exp(-130\,500/RT)$ (m^2 s^{-1}) for Mg diffusion in Al [31] was used as a first approximation since Mg is the major alloying element of the present alloy, the critical strain rate showing a transition from the optimum HSRS region to the high strain rate region was about 2 s^{-1} which was almost two orders magnitude higher than that observed experimentally, i.e. 5×10^{-2} s^{-1} as shown in Fig. 7. It indicates that the power law breakdown was unlikely to occur under the present experimental conditions. Second, recrystallization did not occur before starting the test as shown in Fig. 6 and the deformation time was very short at the high strain rate region. For example, it took only $\sim$80 s for 300% elongation at the initial strain rate of 5×10^{-2} s^{-1} for the sample with the gage length of 8 mm (Fig. 8b). The higher strain rates are imposed, the more hardly dynamic recrystallization occurs due to a lack of time during the testing. It leads to difficulty of grain boundary sliding. Resultantly, the second possibility would be the primary cause for the limited e_f and the low m value at the high strain rate region.

At the low strain rate region, the deformation time was relatively long enough for recrystallization and subsequent grain growth. It took 45 min for 200% elongation at the initial strain rate of 1×10^{-3} s^{-1}. As expected, the microstructure was heterogeneous with coexistence of coarse and fine recrystallized grains as shown in Fig. 11. In addition, cavitation was extensive. This microstructural evolution primarily resulted in the low values of m and e_f at the low strain rate region. Although Sc is a strong microstructure stabilizer, grain growth would be anticipated to occur since the testing temperature of 773 K is over 0.9 of the incipient melting temperature.

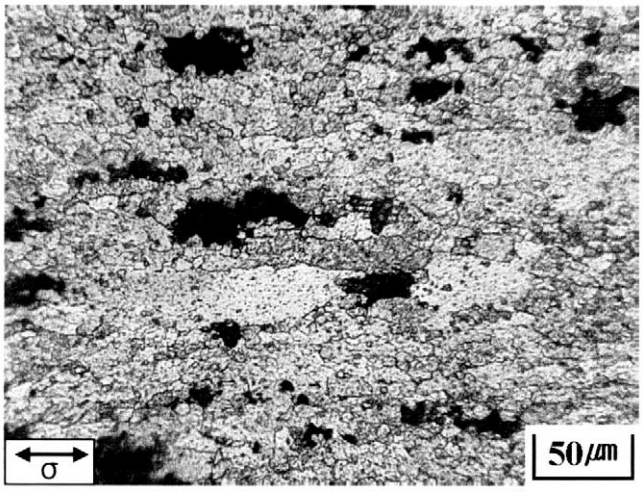

Fig. 11. Microstructure of the as-ECAPed 5083Al+0.2Sc alloy tested at 773 K and 1×10^{-3} s^{-1} (the low strain rate region). The presence of cavity stringers parallel to the tensile axis and the coexistence of coarse and fine recrystallized grains are evident.

4.2. Engineering significance

In the actual superplastic forming process with the superplastic Al alloys, the required strain is about 200% and rarely exceeded 300%. In the present study, the e_f was exceeded 200% in the strain rate range of 1×10^{-3}–5×10^{-1} s^{-1} satisfying the HSRS specification. Additionally, the optimum forming rate is usually one order of magnitude faster than the optimum uniaxial tensile strain rate [32]. Specifically, for conventional superplastic 5083 Al, the optimum uniaxial tensile strain and forming rates are 8×10^{-4} and 8×10^{-3} s^{-1}, respectively and the corresponding forming time for strain of 200% are 40 and 16 min, respectively [32]. Accordingly, by using the present submicrometer grained 5083Al+0.2Sc alloy, the optimum forming rate can be shifted to as fast as 1×10^{-2}–5 s^{-1} and the forming time can be reduced less than 1 min. With regard to compositional modification by adding Sc, as indicated by Furukawa et al. [33], the engineering advantage lies in the fact that only a small amount of Sc addition, for example 0.2 wt.% in the present study, is enough to achieve HSRS in spite of the high cost of raw Sc. For the application of the ECAP process for obtaining an ultrafine grained structure, two aspects are considerable. Although Yamashita et al. [34] reported that 8-passes repetitive pressing with the route B_c resulted in the best microstructure showing the largest elongation, the present result showed that 4-passes pressing is enough to achieve the practical HSRS for the 5083 Al alloy, reducing the material preparation process greatly. Conversely, if higher e_f is required, more repetitive pressing to achieve more finer grain structure with high angle grain boundaries can be applicable since the initial dimension of the sample does not vary during ECAP.

5. Summary

(1) HSRS of the 5083 Al alloy was examined by introducing a ultrafine grained structure of 0.3 μm through ECAP and by adding a small amount of Sc as a microstructure stabilizer.

(2) The ultrafine grained 5083 Al alloy containing Sc was more thermally-stable than the ultrafine grained 5083 Al alloy without Sc processed by the identical preparation method due to the retardation effect of Sc

on recovery and recrystallization associated with the formation of extremely fine Al_3Sc particles.

(3) From a series of tensile tests, the optimum temperature showing HSRS was determined as 773 K. The mechanical behavior of the alloy at 773 K was manifested by a sigmoidal behavior in a double logarithmic plot of the maximum true flow stress against the true strain rate. The maximum elongation to failure of 740% was obtained at 1×10^{-2} s^{-1}. The microstructural examination revealed that HSRS of the alloy was attributed to dynamic recrystallization and preservation of fine recrystallized grains.

(4) Under the optimum high strain rate superplasticitic conditions, failure occurred abruptly in a brittle manner associated with cavitation. During deformation, cavity stringers parallel to the tensile axis were formed by interlinkage of jagged-shaped individual cavities along grain boundaries aligned to the tensile axis.

Acknowledgements

This work was supported by Korea Ministry of Science and Technology through '2000 National Research Laboratory Program'.

References

[1] R.L. Hecht, K. Kannan, in: A.K. Gosh, T.R. Bieler (Eds.), Superplasticity and Superplastic Forming, TMS, Warrendale, PA, USA, 1995, p. 259.
[2] R. Verma, A.K. Gosh, S. Kim, C. Kim, Mater. Sci. Eng. A191 (1995) 143.
[3] R. Verma, P.A. Friedman, A.K. Gosh, S. Kim, C. Kim, Metall. Mater. Trans. 27A (1996) 1189.
[4] P.A. Friedman, A.K. Gosh, Metall. Mater. Trans. 27A (1996) 3827.
[5] Y. Wu, L.D. Castillo, E.J. Lavernia, Metall. Mater. Trans. 28A (1997) 1059.
[6] S.N. Patankar, T.M. Jen, Scripta Mater. 38 (1998) 1255.
[7] D.H. Bae, A.K. Gosh, Acta Mater. 48 (2000) 1207.
[8] I.C. Hsiao, J.C. Huang, Scripta Mater. 40 (1999) 697.
[9] V.M. Segal, V.I. Reznikov, A.D. Drobyshevsky, V.I. Kopylov, Russ. Metall. 1 (1981) 99.
[10] V.M. Segal, Mater. Sci. Eng. A197 (1995) 157.
[11] J. Wang, M. Furukawa, Z. Horita, M. Nemoto, R.Z. Valiev, T.G. Langdon, Mater. Sci. Eng. A216 (1996) 41.
[12] R.R. Sawtell, C.L. Jensen, Metall. Trans. 21A (1990) 421.
[13] L.S. Kramer, W.T. Tack, M.T. Fernandes, Adv. Mater. Proc. (1997) 23 (October).
[14] L.S. Toropova, D.G. Eskin, M.L. Kharakterova, T.V. Dobatkina, Advanced Aluminum Alloys Containing Scandium: Structure and Properties, Gondon and Breach Sci. Pub, Amsterdam, Netherlands, 1998, p. 115.
[15] M. Nemoto, Z. Horita, M. Furukawa, T.G. Langdon, Metals Mater. 4 (1998) 1181.
[16] D.H. Shin, B.C. Kim, Y.-S. Kim, K.-T. Park, Acta Mater. 48 (2000) 2247.
[17] N. Blake, M.A. Hopkins, J. Mater. Sci. 20 (1985) 2861.
[18] R.W. Hyland, Jr., Metall. Trans. 23A (1992) 1947.
[19] Y.-L. Wu, F.H. Froes, C. Li, A. Alvalez, Metall. Mater. Trans. 30A (1999) 1017.
[20] E.A. Marquis, D.N. Seidman, Acta Mater. 49 (2001) 1909.
[21] Glossary of Terms used in Metallic Superplastic Materials, JIS H 7007, Japanese Standards Association, Tokyo, 1995, p. 3.
[22] M. Mabuchi, K. Higashi, Acta Mater. 47 (1999) 1915.
[23] Z. Horita, D.J. Smith, M. Furukawa, M. Nemoto, R.Z. Valiev, T.G. Langdon, J. Mater. Res. 11 (1996) 1881.
[24] R.Z. Valiev, R.K. Islamgaliev, I.V. Alexandrov, Prog. Mater. Sci. 45 (2000) 103.
[25] A. Shan, I.G. Moon, H.S. Ko, J.W. Park, Scripta Mater. 41 (1999) 353.
[26] C.H. Cáceres, D.S. Wilkinson, Acta Metall. 32 (1984) 415.
[27] J. Xinggang, C. Jianchong, M. Longxiang, Acta Metall. Mater. 41 (1993) 2721.
[28] J. Xinggang, J.C. Earthman, F.A. Mohamed, J. Mater. Sci. 29 (1994) 5499.
[29] D.H. Shin, K.-T. Park, Mater. Sci. Eng. A268 (1999) 55.
[30] O.D. Sherby, P.M. Burke, Prog. Mater. Sci. 13 (1967) 325.
[31] S.J. Rothman, N.J. Peterson, L.J. Lowicki, L.C. Robinson, Phys. Status Solidi 63 (1974) 20.
[32] A.J. Barnes, Mater. Sci. Forum 304–306 (1999) 785.
[33] M. Furukawa, A. Utsunomiya, K. Matsubara, Z. Horita, T.G. Langdon, Acta Mater. 49 (2001) 3829.
[34] A. Yamashita, Z. Horita, T.G. Langdon, Mater. Sci. Eng. A300 (2001) 142.